JCTC Journal of Chemical Theory and Computation

Computational DFT Study of Ruthenium Tetracarbonyl Polymer

Mika Niskanen, Pipsa Hirva,* and Matti Haukka

Department of Chemistry, University of Joensuu, P.O. Box 111, FI-80101 Joensuu, Finland

Received September 29, 2008

Abstract: Ruthenium tetracarbonyl polymer, $[Ru(CO)_4]_n$, a chainlike compound formed by metal−metal interactions, was studied computationally. We first performed tests with selected pure and hybrid GGA density functionals and ab initio methods at HF and MP2 levels of theory to find the most suitable method. Calculated geometries and molecular orbitals were compared to see effectiveness and possible differences of the methods. Hybrid functionals, especially PBE1PBE and MPW1K, were found to produce accurate geometrical parameters compared to the experimental structure, with reasonable computational cost. Bonding in $[Ru(CO)_4]_n$ chains was studied by calculation of Mayer bond order and theoretical structure factors followed by multipole refinement to get bond critical points according to the quantum theory of atoms in molecules. Ruthenium−ruthenium bonding comparable to that in a $Ru_3(CO)_{12}$ cluster was found with both methods.

1. Introduction

Chainlike compounds having a transition-metal backbone have been intensively studied in recent years. Interest toward these compounds comes from the various properties these one-dimensional chains exhibit: luminescence,[1] solvatochromy[2] and vapochromy,[3] antitumor activity in "platinum blue"-type compounds,[4,5] and catalytic properties in ruthenium chains containing carbonyl ligands.[6,7] Certain transition-metal chain compounds are also semiconductors with use in electronic devices.[8]

Depending on their structure, chain compounds with metal backbone can be divided into different categories. Square planar metal complexes can form stacks where metal atoms line up. This is the case with, for example, Magnus' green salt,[9,10] its derivatives,[11] and many tetracyanoplatinates.[12] One-dimensional coordination polymers do not have real metal backbone. Instead, they have an alternating chain of metal atoms and linking ligands.[13] In supported chains, including EMACs, metal atom chains are surrounded and held together by bridging ligands.[14] Unsupported chains have metal backbone formed by direct metal−metal interactions without aid from the ligands.[15]

The $[Ru(CO)_4]_n$ polymer is an unsupported chain. It was synthesized for the first time by photolysis from concentrated Ru_3CO_{12} solution in tetrahydrofuran using CO atmosphere in the mid 1980s,[16] and the structure was solved in the beginning of the 1990s.[17] Many of the known chainlike transition-metal structures are mixed valence chains or have charges. $[Ru(CO)_4]_n$, however, is neutral, and all ruthenium atoms have the same valence, making the chain rare and interesting.

Most of the previous studies on the unsupported transition-metal chains focus on experimental work. These studies include synthesis,[18] X-ray studies,[15] electrocatalytic properties,[7,19,20] and spectroelectrochemical studies[21] on similar unsupported ruthenium- and osmium-based chains. Computational work includes a study of ruthenium and osmium chain growth from mononuclear $[M(CO)_4Cl_2]$ units and trinuclear $[M_3(CO)_{12}]$ clusters (M = Ru, Os).[22]

The aim of our study was to examine the $[Ru(CO)_4]_n$ polymer and its properties by means of computational chemistry. We tested the efficiency of various modeling methods suitable for modeling unsupported metal chain structures. We selected nine popular density functionals and also traditional wave functional methods on modeling single chains of $[Ru(CO)_4]_n$ polymer. Additionally, we studied bonding by calculating Mayer bond orders and by multipole

* Corresponding author e-mail: pipsa.hirva@joensuu.fi.

10.1021/ct800407h CCC: $40.75
Published on Web 03/02/2009

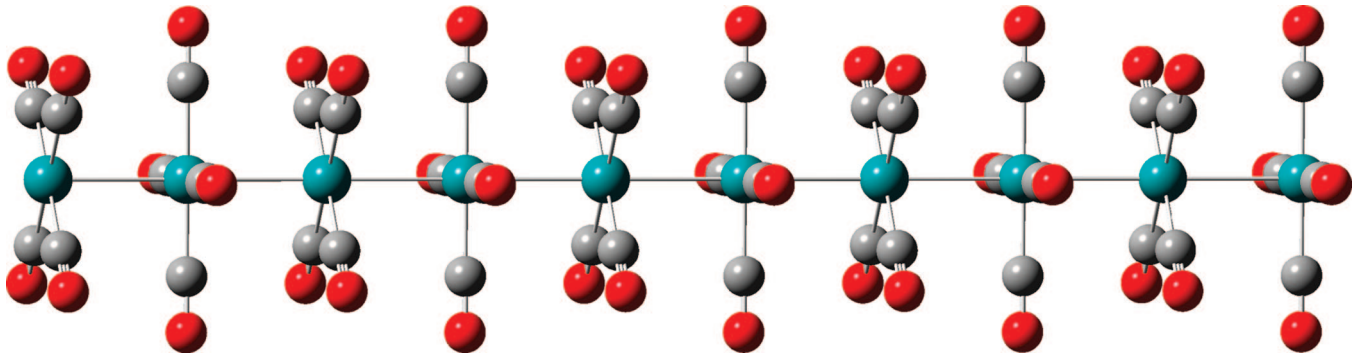

Figure 1. Ten-units-long single chain of $[Ru(CO)_4]_n$. Ru−Ru bond length is 2.86 Å, and C−Ru−Ru−C dihedral angle is 45°.

refinement from calculated theoretical structure factors to locate bond critical points according to the quantum theory of atoms in molecules.[23]

2. Computational Methods

Single chain calculations were carried out with the Gaussian03 program package.[24] Initial geometry tests were made with selected pure GGA density functionals (HCTH,[25] PBEPBE,[26] and VSXC[27]) and hybrid GGA density functionals (B1B95,[28] B3LYP,[29−31] B3PW91,[29,32] B97-2,[33] MPW1K,[34,35] and PBE1PBE[26]). For further studies, we used B1B95, B3PW91, and PBE1PBE (also known as PBE0) functionals. Ab initio calculations with HF and MP2 levels of theory were also performed for comparison. Two different basis sets were tested for ruthenium atom: Huzinaga's all-electron basis set[36] with an additional p-polarization function (433321/4331/421) and Los Alamos National Laboratory 2-double-ζ (LanL2DZ).[37] The latter is a small core ECP basis set, with 16 valence electrons for ruthenium atom, and incorporates mass−velocity and Darwin relativistic effects into the potentials. The basis set used for nonmetal atoms was the standard all-electron basis set 6-31G(d), but effects of increasing it to 6-311+G(d) were also tested. Symmetry was utilized in all models to speed up calculations. Frequency calculations with no scaling were performed to ensure all optimized molecular structures were minima.

For 3D periodic calculations, we used the CRYSTAL program package.[38] Calculations were performed with the PBE1PBE hybrid functional. Basis sets for C[39] and O[40] were selected from the CRYSTAL basis set library. For ruthenium, we used an all-electron basis set developed for the free atom case[41] and modified it for solid-state calculations by removing the most diffuse functions. The final basis set had a contraction of 976311/76311/631.

3. Results and Discussion

3.1. Molecular Models. Models of $[Ru(CO)_4]_n$ chains were based on crystallography information.[17] Our initial testing models were single chain models; interactions between $[Ru(CO)_4]_n$ chains are weak so neighboring chains from crystal structure were excluded for simplicity (Figure 1).

In powder X-ray study, $[Ru(CO)_4]_n$ polymer had been estimated to be roughly an average of 90 monomers long.[17] We built multiple short models $[Ru(CO)_4]_n$ (n = 2, 3, 4, 6, 8, 10) and tested hydrogen, chloride, water, and carbonyl ligands for terminating ends of the models. We also tested a model without a terminating group. Terminating the chain with carbonyl distorted the geometry at the ends of the chain. Water as terminating group constrained symmetry, which was not to our best interest. Effects of the other tested terminating groups on Ru−Ru distance in the middle of the chain can be seen in Figure 2. In longer chains, the effect of terminating group diminished. Ru−Ru distance approached approximate value of 2.88 Å which is in good agreement with the X-ray measured value of 2.86 Å in the crystal. We decided to use nonterminated $[Ru(CO)_4]_n$ chain models for our studies. This way, models were simpler and stabilization energies could be compared reliably.

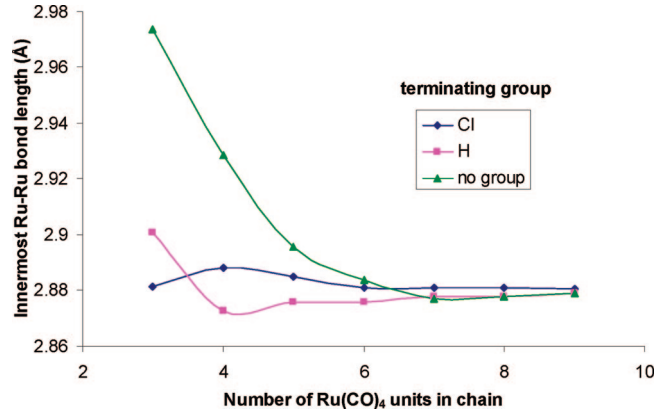

Figure 2. Effect of chain length and terminating group on the innermost Ru−Ru bond length (B3PW91, Huzinaga's AE basis set for ruthenium).

3.2. Tests for Functionals. Functionals were first tested by partial optimization of chains with selected Ru−Ru distances. We made the tests with small models, $[Ru(CO)_4]_n$ (n = 2, 3, 4), where Ru−Ru distances were fixed between values of 2.70 and 3.40 Å with 0.02 or 0.04 Å increments. Selected results for relative energies as a function of Ru−Ru distance can be seen in Figure 3. With VSXC functional, energy rose only slightly when the Ru−Ru bond was lengthened, indicating that the energy minimum could not be found easily. HCTH did better, but energy still increased more slowly than with PBEPBE or its hybrid counterpart PBE1PBE. All the hybrid functionals gave a curve similar to that of PBE1PBE. Moreover, hybrid functionals converged easily, whereas some extra work was needed with pure

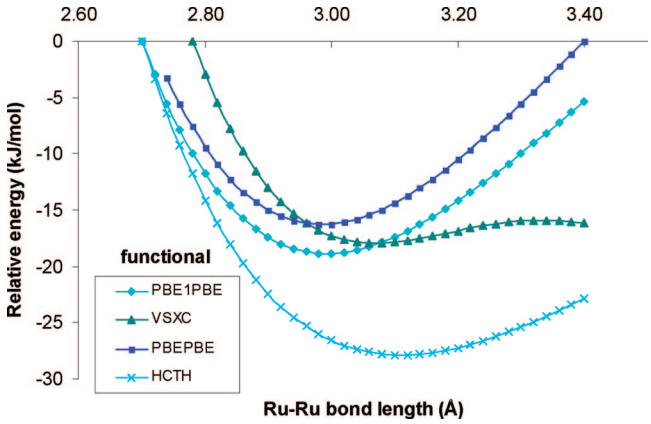

Figure 3. Relative $[Ru(CO)_4]_2$ energies as a function of Ru−Ru bond length. (Huzinaga's AE basis set.) The highest calculated energy with each functional has been set to 0 kJ/mol.

functionals in $n = 3$ and 4 models to reach geometry convergence.

It is not a real surprise that HCTH and VSXC work poorly as it has been noted before that most pure functionals do not work well on transition-metal carbonyl complexes.[42] Therefore, pure functionals were excluded from further studies.

For further testing, we performed full geometry optimizations to longer $[Ru(CO)_4]_n$ ($n = 6, 8, 10$) models using only the tested hybrid functionals and wave functional methods. Innermost Ru−Ru bond lengths for the calculated structures are presented in Table 1.

Many of the hybrid functionals gave results very close to experimental values, namely B3PW91, MPW1K, and PBE1PBE when Huzinaga's AE basis set was used and B1B95, MPW1K, and PBE1PBE when LanL2DZ basis set was used. Changing the metal basis set from Huzinaga's AE to LanL2DZ gave a (systematic) increase of 2−4 pm to Ru−Ru bond lengths with the density functionals. The difference most probably results from the relativistic effects, which the Huzinaga's AE basis set does not account for. However, in our previous tests for different carbonyl complexes of group 8 transition metals (including trinuclear cluster complexes $M_3(CO)_{12}$, M = Fe, Ru, Os), we showed that the relativistic effects are rather small for the 4d elements, both in geometry and in decarbonylation energies.[42] The very stable Huzinaga's basis set was found especially suitable for studying ruthenium carbonyl complexes.

The Hartree−Fock method also reproduced the overall geometry of chains well, but the bond distances were quite far from the experimental values and values of DFT methods. Results obtained by the MP2 method were in good agreement with DFT methods and experimental values for innermost Ru−Ru and Ru−C lengths, but neighboring $Ru(CO)_4$ units are no longer strictly square planar. Furthermore, the computation requirements were considerably higher with the MP2 method, taking roughly 450 times longer than DFT calculations and effectively prohibiting the calculation of longer chains than $[Ru(CO)_4]_8$.

Effects of improving the nonmetal atom basis set to 6-311+G(d) were also tested. Geometries were slightly affected; Ru−Ru bonds were 1 to 2 pm longer and C−O bonds were about 1 pm shorter. However, these changes occurred with all the functionals and did not change their relative results.

$[Ru(CO)_4]_n$ chains with 6−10 units had similar geometry in the central parts of the chain as the real polymers of about 90 units. To see the effect of extending the size of the model, we calculated a one-dimensional periodic single chain describing an infinite polymer, $[Ru(CO)_4]_\infty$.

Obtained bond lengths are shown in Table 2. Optimizations of infinite chains with Huzinaga's AE basis set reproduced the results of longest finite chains with differences less than 1 pm. Again, the most accurate geometry was obtained with the PBE1PBE and MPW1K functionals.

Stabilization energies were calculated with chosen functionals. The energies were calculated using equation $E_{stab} = (E_n/n) - E_1$, where E_n/n is the energy of an n-units-long chain divided by the number of units and E_1 is the energy of a single $Ru(CO)_4$ unit. Results are shown in Figure 4.

The chosen functionals gave similar results with a difference around 15 kJ/mol between PBE1PBE and B3PW91. The energy difference between chains of 9 and 10 units was only 3−4 kJ/mol, and thus the energies were slowly approaching their limiting values.

Ruthenium complexes, which follow the 18-electron rule, usually exhibit a singlet ground state. However, in the case of unsaturated systems, optimizing the spin state can lead to different electronic states, which are close in energy.[43] In our molecular models, the effect can be expected to be the largest at the end groups of the chains, since both of the $Ru(CO)_4$ units are 17-electron systems. The triplet spin state was calculated for the nonterminated models with the PBE1PBE/Huzinaga method, which was found to produce reliable results for the singlet state. In the monomer and dimer, the singlet state was found energetically favored. However, as the chain increased, the energy of the triplet decreased, as can be seen in the stabilization energies in Figure 4. On the other hand, since the central $Ru(CO)_4$ units are saturated, the effect of the end groups converged with increasing the size of the chain. Additionally, the effect of optimizing the spin state was found to have a negligible effect on the optimized geometry parameters of the longer chains ($\Delta d = 0.0005$ Å for the central Ru−Ru bond in $[Ru(CO)_4]_8$).

3.3. Properties of $[Ru(CO)_4]_n$. Selected molecular orbitals of $[Ru(CO)_4]_6$ and $[Ru(CO)_4]_8$ models were calculated and examined with B1B95, B3PW91, and PBE1PBE functionals. The orbitals between HOMO−9 and LUMO+9 and their relative energy levels were almost identical regardless of the functional or metal basis set used. In general, the orbitals were highly delocalized along the chain. As an example, we have drawn selected molecular orbitals delocalized over metal chain (Figure 5a,b) and along the entire molecule (Figure 5c,d). In Figure 5a,b, we can see Ru−Ru bonding and antibonding interactions. We further examined the nature of the M−M bonding with NBO analysis, which revealed that the Ru−Ru bonds consisted mainly of d−d interactions with 25−30% of s and 70−75% of d_{z^2} character.

Table 1. Optimized Structure of $[Ru(CO)_4]_8$ Calculated with Various DFT Methods, HF, and MP2 Method[a]

bond	B1B95	B3LYP	B3PW91	B97-2	MPW1K	PBE1PBE	HF	MP2	exptl[17]
				Huzinaga AE					
Ru−Ru	2.825	2.919	2.878	2.896	2.837	2.849	2.959	2.858	2.860
	−1.2%	2.1%	0.63%	1.3%	−0.80%	−0.38%	3.5%	−0.07%	
Ru−C	1.954	1.970	1.955	1.955	1.951	1.951	2.029	1.935	1.951
	0.15%	0.97%	0.21%	0.21%	0.0%	0.0%	4.0%	−0.82%	
C−O	1.144	1.149	1.148	1.147	1.136	1.146	1.118	1.168	1.133
	0.97%	1.4%	1.3%	1.2%	0.27%	1.1%	−1.3%	3.1%	
				LanL2DZ					
Ru−Ru	2.849	2.954	2.908	2.924	2.859	2.874	2.971	2.843	2.860
	−0.38%	3.3%	1.7%	2.2%	0.035%	0.49%	3.9%	−0.59%	
Ru−C	1.952	1.966	1.951	1.952	1.947	1.947	2.019	1.922	1.951
	0.051%	0.77%	0.0%	0.051%	−0.205%	−0.205%	3.5%	−1.5%	
C−O	1.145	1.150	1.149	1.148	1.136	1.147	1.119	1.169	1.133
	1.1%	1.5%	1.4%	1.3%	0.24%	1.2%	−1.2%	3.2%	

[a] Bond lengths are in angstroms. Percent values are deviations from the experimental value.

Table 2. Optimized Structure of $[Ru(CO)_4]_\infty$ Calculated with HF and Selected DFT Methods[a]

bond	B1B95	B3LYP	B3PW91	B97-2	MPW1K	PBE1PBE	HF	exptl[17]
				Huzinaga AE				
Ru−Ru	2.826	2.923	2.880	2.896	2.838	2.851	2.962	2.860
	−1.2%	0.97%	1.3%	1.3%	−0.77%	−0.31%	3.6%	
Ru−C	1.954	1.970	1.955	1.955	1.951	1.951	2.028	1.951
	0.5%	0.97%	0.21%	0.21%	0.0%	0.0%	3.9%	
C−O	1.144	1.149	1.148	1.147	1.136	1.146	1.118	1.133
	0.97%	1.4%	1.3%	1.2%	0.26%	1.1%	−1.3%	

[a] Bond lengths are in angstroms. Percent values are deviations from the experimental value.

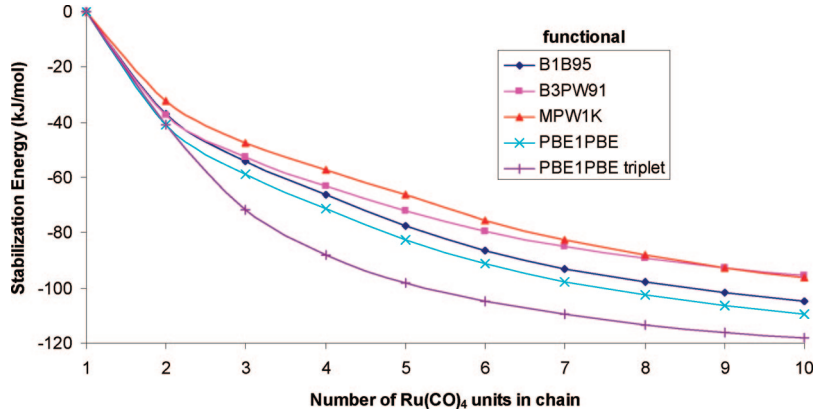

Figure 4. Stabilization energies with chosen functionals.

According to a previous study of compounds with staggered and eclipsed carbonyl groups,[45] staggered conformation maximizes the 1,3 M···C interactions and strengthens M−M bonding. This was also discussed in a powder X-ray study.[17] In our study, it is possible to see bonding 1,3 M···C and 1,4 C···C interactions in calculated molecular orbitals, as shown in Figure 5c,d. These interactions can be observed with only low cutoff values, however, which suggests that their effect on bonding between adjacent $Ru(CO)_4$ units will be minor even if bonding interactions exist.

We wanted to study closer the nature of bonding and interactions in $[Ru(CO)_4]_n$ chains. For this, we calculated Mayer bond orders[46] in the $[Ru(CO)_4]_8$ chain using QMForge.[47] Mayer bond orders in the $Ru_3(CO)_{12}$ cluster were calculated for comparison. Selected results are shown in Table 3.

According to Mayer bond orders, direct Ru−Ru bonding in chains is stronger than that in the $Ru_3(CO)_{12}$ cluster despite similar bond lengths. However, there are six weak 1,3 Ru···C interactions with MBO of 0.11 in a cluster that may strengthen overall bonding by forming weak bridges. Mayer bond orders obtained for 1,3 Ru···C interactions in the $[Ru(CO)_4]_8$ chain were negligible. Even though there are eight of these kinds of interactions between each $Ru(CO)_4$ unit, their contribution to bonding seems to be small or nonexistent, according to our study.

It should be noted that the $Ru_3(CO)_{12}$ cluster was calculated in gas phase and CO groups were in staggered conformation. In an X-ray study[48] the axial CO groups were found to be in eclipsed conformation, favoring 1,4 C···C interactions. However, the eclipsed conformation in the cluster is due to packing effects in solid state, and information on the Mayer bond orders in the single molecule in staggered conformation can be used for comparison with the polymeric chain.

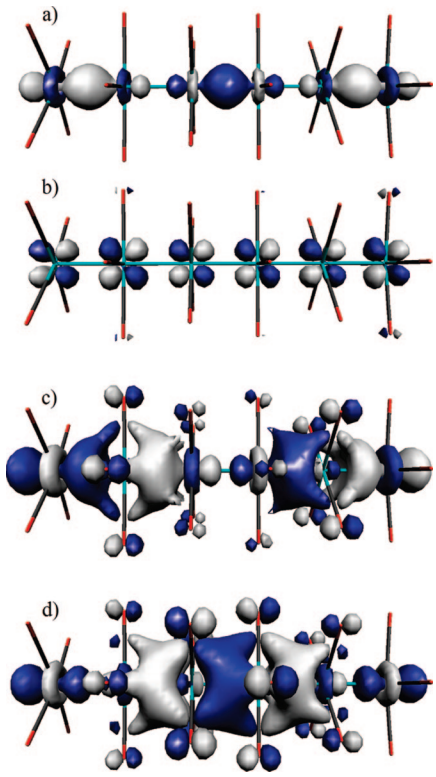

Figure 5. Selected molecular orbitals for $[Ru(CO)_4]_6$. (a) H-7, (b) H-4, (c) H-2, and (d) H-1. A cutoff value of 0.04 was used in (a) and (b), and a cutoff value of 0.02 was used in (c) and (d). Visualization was done with MOLEKEL 4.3.[44]

Table 3. Selected Mayer Bond Orders

atom pair	MBO in $[Ru(CO)_4]_8$	MBO in $Ru_3(CO)_{12}$
Ru−Ru	0.70	0.62
Ru−C	0.88	0.87;[a] 0.94[b]
C−O	2.1	2.1;[a] 2.2[b]
1,3 Ru···C	0.03	0.11;[c] 0.01−0.02
1,4 C···C	0.01	0.02

[a] Axial carbons. [b] Equatorial carbons. [c] 1,3 Ru···C interactions to two axial carbons, bonded on different ruthenium atoms.

3.4. Properties of $[Ru(CO)_4]_n$ Based on 3D Periodic Model. Our second periodic model was a real three-dimensional crystal structure where the neighboring chains were included. Parameters for unit cell and atomic positions were taken from powder X-ray data[17] and optimized using the PBE1PBE functional and CRYSTAL program package.[38] A one-dimensional chain was calculated for comparison. $[Ru(CO)_4]_n$ crystal packing and unit cell borders are shown in Figure 6, and selected structural parameters are shown in Table 4. The optimized unit cell was slightly smaller than the experimental value. However, the overall structure was very well reproduced. 1D and 3D models gave similar Ru−Ru lengths and C−Ru−Ru−C dihedral angles, indicating that the interchain interactions have only a small effect on the geometry of the chains.

Finally, we used CRYSTAL to calculate theoretical structure factors for our optimized 3D periodic crystal structure of $[Ru(CO)_4]_n$ and made multipole refinement with XD2006[49] for the obtained data. Bond critical points, shown

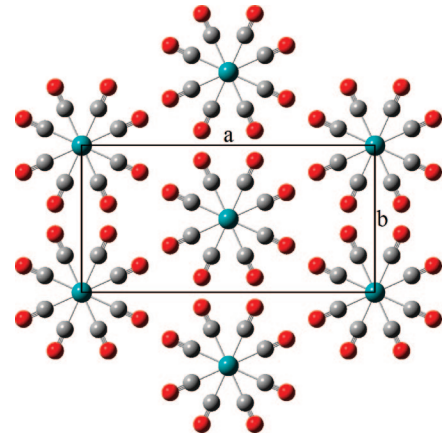

Figure 6. $[Ru(CO)_4]_n$ unit cell and crystal packing.

Table 4. $[Ru(CO)_4]_n$ Structural Parameters

parameter	optimized 1D	optimized 3D	powder X-ray[17]
a		13.94 Å	14.15 Å
b		6.85 Å	7.06 Å
c	5.62 Å	5.64 Å	5.72 Å
Ru−Ru	2.81 Å	2.82 Å	2.860 Å
Ru−C	1.94 Å	1.94 Å	1.951 Å
C−O	1.15 Å	1.15 Å	1.133 Å
C−Ru−Ru−C	44.7°	39.8°	41.0°

in Table 5, were calculated using Bader's quantum theory of atoms in molecules[23] approach, which provides information about atoms and bonding through charge density analysis. This kind of indirect route to topological analysis has been suggested to reduce differences between theory and experiment.[50] Obtained charge density, $\rho(\mathbf{r})$, its Laplacian, $\nabla^2\rho(\mathbf{r})$, kinetic energy density, $G(\mathbf{r})$, potential energy density, $V(\mathbf{r})$, and total energy density, $H(\mathbf{r})$, were compared to values in the experimental charge density study of the $Ru_3(CO)_{12}$ cluster.[48]

The interactions between atoms can be classified on the basis of the sign of the $\nabla^2\rho(\mathbf{r})$ at bond critical point. Negative value means charge is locally concentrated and electrons are shared by both nuclei, which is typical, for example, for covalent interactions (shared shell interactions). Positive value suggests charge is locally depleted and electrons are concentrated in each atom, which is typical, for example, for ionic bonds (closed shell interactions). Further information about the bond can be obtained from energy density values $G(\mathbf{r})$, $V(\mathbf{r})$, and $H(\mathbf{r})$ at bond critical point. These can be calculated from ρ_{BCP} and $\nabla^2\rho_{BCP}$.[51,52] Espinosa et al.[53] further classified interatomic interactions to three categories using the energy density values: pure closed shell interactions ($\nabla^2\rho_{BCP} > 0$, $H_{BCP} > 0$), transit closed shell interactions ($\nabla^2\rho_{BCP} > 0$, $H_{BCP} < 0$), and pure shared shell interactions ($\nabla^2\rho_{BCP} < 0$, $H_{BCP} < 0$). Metal−metal bonds fall in the transit closed shell category, as a typical M−M bond has a low ρ_{BCP}, low and positive $\nabla^2\rho_{BCP}$, and H_{BCP} negative and close to zero.[54]

The values of ρ_{BCP} and $\nabla^2\rho_{BCP}$ in Ru−Ru, Ru−C, and C−O bonds in the $[Ru(CO)_4]_n$ polymer were very similar to corresponding values in the $Ru_3(CO)_{12}$ cluster. The Ru−Ru bonds in $[Ru(CO)_4]_n$ have the typical ρ_{BCP}, $\nabla^2\rho_{BCP}$, and H_{BCP}

Table 5. Selected Parameters in Bond Critical Points[a]

bond critical point	R (Å)	R_{BCP} (Å)	ρ_{BCP} (e Å^{-3})	$\nabla^2\rho_{BCP}$ (e Å^{-5})	G_{BCP} (hartree Å^{-3})	V_{BCP} (hartree Å^{-3})	H_{BCP} (hartree Å^{-3})
				$[Ru(CO)_4]_n$, Optimized			
Ru−Ru	2.819	1.409	0.217	2.33	0.17	−0.18	−0.01
Ru−C	1.938	1.041	0.903	11.2	1.2	−1.6	−0.4
C−O	1.150	0.418	3.440	−39.0	4.5	−11.7	−7.2
1,4 C···C	not found						
1,3 Ru···C	not found						
				$Ru_3(CO)_{12}$, Experimental[48]			
Ru−Ru	2.852	1.425	0.215	2.21	0.17	−0.18	−0.01
Ru−C_{ax}	1.943	1.073	0.903	11.4	1.2	−1.6	−0.4
Ru−C_{ekv}	1.924	1.065	0.985	11.3	1.3	−1.8	−0.5
C−O	1.140	0.442	3.8	−45	5	−14	−9
1,4 C···C	2.815	1.439	0.12	0.99	0.07	−0.07	0.00
1,3 Ru···C	not found						

[a] All shown values are averages. R = distance between atoms, R_{BCP} = distance between first mentioned atom and bond critical point.

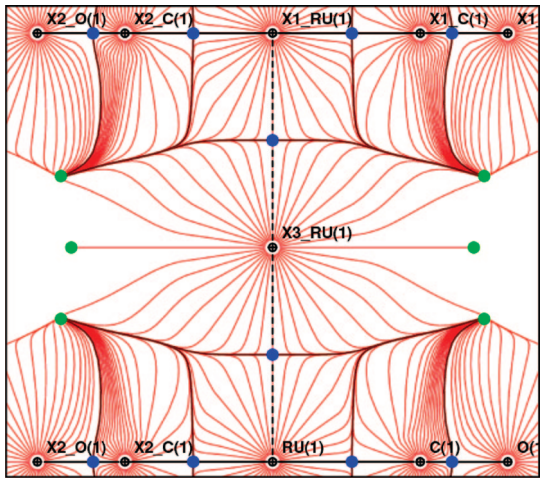

Figure 7. Trajectories with bond critical points (blue) and ring critical points (green) for optimized $[Ru(CO)_4]_n$ 3D model.

values for the M−M bond and belong to the transit closed shell category. Plotted trajectories can be seen in Figure 7. We could not find evidence of 1,3 M···C bonding in the polymer. The possible 1,3 M···C interactions are likely to be too weak to have bond critical points and thus do not play a role in bonding along the Ru chain.

4. Conclusions

Various DFT functionals as well as ab initio methods were tested for modeling ruthenium tetracarbonyl polymer, $[Ru(CO)_4]_n$. Hybrid functionals seem to work well for modeling $[Ru(CO)_4]_n$ in either single chains or crystal state. Functionals PBE1PBE and MPW1K gave especially accurate results. We expect these functionals to perform well with other similar Ru-based linear metal chains such as $[Ru(bpy)(CO)_2]_n$. It is also noteworthy that the model does not need to be longer than six units to obtain geometry and results similar to longer chains.

Mayer bond orders were calculated and a bond critical point search was performed to study bonding in $[Ru(CO)_4]_n$. From the results, we deduced direct Ru−Ru bonding in $[Ru(CO)_4]_n$ to be similar and about the same strength as that in the $Ru_3(CO)_{12}$ cluster. However, overall bonding is stronger in the cluster because of additional interactions from carbonyls. The bonding studies also give a point of comparison for the future when similar chains will be computed. The computational approach and theoretical structure factors may also serve as an aid in the interpretation of experimental data, when satisfactory data is difficult or impossible to get.

Acknowledgment. We thank Matti Tuikka for his comments and advice on charge density studies. The Academy of Finland is gratefully acknowledged for financial support.

References

(1) Stender, M.; White-Morris, R. L.; Olmstead, M. M.; Balch, A. *Inorg. Chem.* **2003**, *42*, 4504.

(2) Yam, V. W.-W.; Wong, K. M.-C.; Zhu, N. *J. Am. Chem. Soc.* **2002**, *124*, 6506.

(3) Buss, C. E.; Mann, K. R. *J. Am. Chem. Soc.* **2002**, *124*, 1031.

(4) Tejel, C.; Cirano, M. A.; Oro, L. A. *Chem.−Eur. J.* **1999**, *5*, 1131.

(5) Davidson, J. P.; Faber, P. J.; Fischer, R. G., Jr.; Mansy, S.; Peresie, H. J.; Rosenberg, B.; Van Camp, L. *Cancer Chemother. Rep., Part 1* **1975**, *59*, 287.

(6) Luukkanen, S.; Homanen, P.; Haukka, M.; Pakkanen, T. A.; Deronzier, A.; Chardon-Noblat, S.; Zsoldos, D.; Ziessel, R. *Appl. Catal., A* **1994**, *185*, 157.

(7) Collomb-Dunand-Sauthier, M.-N.; Deronzier, A.; Ziessel, R. *Inorg. Chem.* **1994**, *33*, 2961.

(8) Caseri, W. R.; Chanzy, H. D.; Feldman, K.; Fontana, M.; Smith, P.; Tervoort, T. A.; Goossens, J. G. P.; Meijer, E. W.; Schenning, A. P. H. J.; Dolbnya, I. P.; Debije, M. G.; de Haas, M. P.; Warman, J. M.; van de Craats, A. M.; Friend, R. H.; Sirringhaus, H.; Stutzmann, N. *Adv. Mater.* **2003**, *15*, 125.

(9) Atoji, M.; Richardson, J. W.; Rundle, R. E. *J. Am. Chem. Soc.* **1957**, *79*, 3017.

(10) Kim, E.-G.; Schmidt, K.; Caseri, W. R.; Kreouzis, T.; Stingelin-Stutzmann, N.; Brédas, J. L. *Adv. Mater.* **2006**, *18*, 2039.

(11) Caseri, W. *Platinum Met. Rev.* **2004**, *48*, 91.

(12) Loosli, A.; Wermuth, M.; Güdel, H.-U.; Capelli, S.; Hauser, J.; Bürgi, H.-B. *Inorg. Chem.* **2000**, *39*, 2289.

(13) Benmansour, S.; Setifi, F.; Gómez-García, C. J.; Triki, S.; Coronado, E. *Inorg. Chim. Acta* **2008**, *361*, 3856.

(14) Berry, J. F.; Cotton, F. A.; Fewox, C. S.; Lu, T.; Murillo, C. A.; Wang, X. *Dalton Trans.* **2004**, *15*, 2297.

(15) Masciocchi, N.; Sironi, A.; Chardon-Noblat, S.; Deronzier, A. *Organometallics* **2002**, *21*, 4009.

(16) Hastings, W. R.; Baird, M. C. *Inorg. Chem.* **1986**, *25*, 2913.

(17) Masciocchi, N.; Moret, M.; Cairati, P.; Ragaini, F.; Sironi, A. *J. Chem. Soc., Dalton Trans.* **1993**, *3*, 471.

(18) Jiang, F.; Yap, G. P. A.; Pomeroy, R. K. *Organometallics* **2002**, *21*, 773.

(19) Chardon-Noblat, S.; Collomb-Dunand-Sauthier, M.-N.; Deronzier, A.; Ziessel, R.; Zsoldos, D. *Inorg. Chem.* **1994**, *33*, 4410.

(20) Chardon-Noblat, S.; Deronzier, A.; Hartl, F.; Slageren, J.; Mahabiersing, T. *Eur. J. Inorg. Chem.* **2001**, *3*, 613.

(21) Hartl, F.; Mahabiersing, T.; Chardon-Noblat, S.; Da Costa, P.; Deronzier, A. *Inorg. Chem.* **2004**, *43*, 7250.

(22) Hirva, P.; Haukka, M.; Jakonen, M.; Pakkanen, T. A. *Inorg. Chim. Acta* **2006**, *359*, 853.

(23) Bader, R. F. W. In *Atoms in Molecules: A Quantum Theory*; Clarendon Press: Oxford, 1990.

(24) Frisch, M. J.; Trucks, G. W.; Schlegel, H. B.; Scuseria, G. E.; Robb, M. A.; Cheeseman, J. R.; Montgomery, J. A., Jr.; Vreven, T.; Kudin, K. N.; Burant, J. C.; Millam, J. M.; Iyengar, S. S.; Tomasi, J.; Barone, V.; Mennucci, B.; Cossi, M.; Scalmani, G.; Rega, N.; Petersson, G. A.; Nakatsuji, H.; Hada, M.; Ehara, M.; Toyota, K.; Fukuda, R.; Hasegawa, J.; Ishida, M.; Nakajima, T.; Honda, Y.; Kitao, O.; Nakai, H.; Klene, M.; Li, X.; Knox, J. E.; Hratchian, H. P.; Cross, J. B.; Bakken, V.; Adamo, C.; Jaramillo, J.; Gomperts, R.; Stratmann, R. E.; Yazyev, O.; Austin, A. J.; Cammi, R.; Pomelli, C.; Ochterski, J. W.; Ayala, P. Y.; Morokuma, K.; Voth, G. A.; Salvador, P.; Dannenberg, J. J.; Zakrzewski, V. G.; Dapprich, S.; Daniels, A. D.; Strain, M. C.; Farkas, O.; Malick, D. K.; Rabuck, A. D.; Raghavachari, K.; Foresman, J. B.; Ortiz, J. V.; Cui, Q.; Baboul, A. G.; Clifford, S.; Cioslowski, J.; Stefanov, B. B.; Liu, G.; Liashenko, A.; Piskorz, P.; Komaromi, I.; Martin, R. L.; Fox, D. J.; Keith, T.; Al-Laham, M. A.; Peng, C. Y.; Nanayakkara, A.; Challacombe, M.; Gill, P. M. W.; Johnson, B.; Chen, W.; Wong, M. W.; Gonzalez, C.; Pople, J. A. Gaussian 03, revision C.02; Gaussian, Inc.: Wallingford, CT, 2004.

(25) Hamprecht, F. A.; Cohen, A. J.; Tozer, D. J.; Handy, N. C. *J. Chem. Phys.* **1998**, *109*, 6264.

(26) Perdew, J. P.; Burke, K.; Ernzerhof, M. *Phys. Rev. Lett.* **1996**, *77*, 3865.

(27) Van Voorhis, T.; Scuseria, G. E. *J. Chem. Phys.* **1998**, *109*, 400.

(28) Becke, A. D. *J. Chem. Phys.* **1996**, *104*, 1040.

(29) Becke, A. D. *J. Chem. Phys.* **1993**, *98*, 5648.

(30) Lee, C.; Yang, W.; Parr, R. G. *Phys. Rev. B* **1988**, *37*, 785.

(31) Stephens, P. J.; Devlin, F. J.; Chabalowski, C. F.; Frisch, M. J. *J. Phys. Chem.* **1994**, *98*, 11623.

(32) Perdew, J. P. In *Electronic Structure of Solids '91*; Ziesche, P., Eschig, H., Eds.; Akademie Verlag: Berlin, 1991; p 11.

(33) Wilson, P. J.; Bradley, T. J.; Tozer, D. J. *J. Chem. Phys.* **2001**, *115*, 9233.

(34) Becke, A. D. *J. Chem. Phys.* **1997**, *107*, 8554.

(35) Adamo, C.; Barone, V. *J. Chem. Phys.* **1998**, *108*, 664.

(36) *Gaussian Basis Sets for Molecular Calculations*; Huzinaga, S., Ed.; Physical Sciences Data 16; Elsevier: Amsterdam, 1984; p 255.

(37) Hay, P. J.; Wadt, W. R. *J. Chem. Phys.* **1985**, *82*, 299.

(38) Dovesi, R.; Saunders, V. R.; Roetti, C.; Orlando, R.; Zicovich-Wilson, C. M.; Pascale, F.; Civalleri, B.; Doll, K.; Harrison, N. M.; Bush, I. J.; Arco, P. D.; Llunell, M. *CRYSTAL06 User's Manual*; University of Torino: Torino, Italy, 2006.

(39) Catti, M.; Pavese, A.; Dovesi, R.; Saunders, V. C. *Phys. Rev. B* **1993**, *47*, 9189.

(40) Gatti, C.; Saunders, V. R.; Roetti, C. *J. Chem. Phys.* **1994**, *101*, 10686.

(41) Towler, M. D. University of Cambridge, Private communication, 2008.

(42) Hirva, P.; Haukka, M.; Jakonen, M.; Moreno, M. A. *J. Mol. Model.* **2008**, *14*, 171.

(43) Carreon-Macedo, J.-L.; Harvey, J. N. *J. Am. Chem. Soc.* **2004**, *126*, 5789.

(44) Flükiger, P.; Lüthi, H. P.; Portmann, S.; Weber, J. *MOLEKEL 4.3*; Swiss National Supercomputing Centre CSCS: Manno, Switzerland, 2000.

(45) Bau, R.; Kirtley, S. W.; Sorrell, T. N.; Winarko, S. *J. Am. Chem. Soc.* **1973**, *96*, 988.

(46) Bridgeman, A. J.; Cavigliasso, G.; Ireland, L. R.; Rothery, J. *J. Chem. Soc., Dalton Trans.* **2001**, *14*, 2095.

(47) Tenderholt, A. L. QMForge, version 2.1; Stanford University: Stanford, CA, 2007. http://qmforge.sourceforge.net.

(48) Gervasio, G.; Bianchi, R.; Marabello, D. *Chem. Phys. Lett.* **2005**, *407*, 18.

(49) Volkov, A.; Macchi, P.; Farrugia, L. J.; Gatti, C.; Mallinson, P.; Richter, T.; Koritsanszky, T. XD2006, a computer program package for multipole refinement, topological analysis of charge densities and evaluation of intermolecular energies from experimental and theoretical structure factors; SUNY at Buffalo: Buffalo, NY, 2006.

(50) Volkov, A.; Abramov, Y.; Coppens, P.; Gatti, C. *Acta Crystallogr., Sect. A* **2000**, *56*, 332.

(51) Abramov, Yu. *Acta Crystallogr., Sect. A* **1997**, *53*, 264.

(52) Espinosa, E.; Molins, E.; Lecomte, C. *Chem. Phys. Lett.* **1998**, *285*, 170.

(53) Espinosa, E.; Alkorta, I.; Elguero, J.; Molins, E. *J. Chem. Phys.* **2002**, *117*, 5529.

(54) Gervasio, G.; Bianchi, R.; Marabello, D. *Chem. Phys. Lett.* **2004**, *387*, 481.

CT800407H